ADVANCED FUNCTIONAL MATERIALS
www.afm-journal.de

Transport Properties of Polymer Semiconductor Controlled by Ionic Liquid as a Gate Dielectric and a Pressure Medium

*Wu Shi, Jianting Ye, Joseph G. Checkelsky, Chieko Terakura, and Yoshihiro Iwasa**

An effective way of using ionic liquid as a gate dielectric as well as a pressure medium to tune the transport of an exemplary polymer semiconductor, poly(2,5-bis(3-tetradecyl-thiophene-2-yl)thieno[3,2-b]thiophene) (pBTTT-C14) is presented. Working as gate dielectrics, the ionic liquids exhibit the well-known ability to induce dense carriers (>10^{20} cm^{-3}) in the polymer film contributing to the high conductivity (≈10^2 S cm^{-1}). In addition, it is found that the ionic liquid works as a pressure medium at the highly charged state, leading to significant enhancement of conductivity. By combining both gating and pressuring, a crossover of transport properties is observed from one-dimensional to three-dimensional hopping, as the clear indication that the polymer film has accessed the regime adjacent to the transition region between insulator and metal. These results show an effective way of utilizing pressure effect of ionic liquid as a new degree of freedom in controlling transport of polymers, a method having strong potential to be generalized for even broader range of materials.

1. Introduction

Realizing metallic states over a wide temperature range in conjugated polymers has been a long time challenge in the study of polymer based conductors.[1] By chemical doping, polymers can reach relatively high conducting states at room temperature and exhibit a great variety of transport properties.[2–7] At lower temperature, the majority of doped polymers exhibit semiconducting transport characterized by thermally assisted hopping over random localized states.[2–4] However, in chemically doped polypyrrole[5] and polyaniline,[6,7] metallic transport has been reported even at cryogenic temperatures.

To access the metallic transport in polymers, it has been suggested that the high carrier density introduced via chemical doping and improved molecular structure with enhanced π–π interchain stacking plays a key role.[6] Recently, in addition to chemical doping, ultra high density of carriers introduced by electrostatic or electrochemical doping has been studied. The carrier accumulation is mediated by ionic movement in ionic conductors such as polymer electrolytes,[8–13] ion gels,[14–16] or ionic liquids (IL)[17–21] forming narrowly separated (≈1 nm) layers of carriers, called the electric double layer (EDL). Using these narrow dielectrics, an EDL transistor (EDLT) exhibits a unique ability to accumulate high density carriers (>10^{15} charges cm^{-2}) even with low bias voltages.[8,19] Benefited by the high carrier density in EDLTs, a highly conducting or even "metallic" state in the polymers was reported at room temperature.[11–13] Furthermore, a significant advantage for EDLT in contrast to conventional chemical doping[1] is that the doping can be controlled reversibly without causing chemical modification of the polymer structures. Additionally, it is well known that besides the structural improvement by newly developed processing methods,[6] application of high pressure may enhance the π–π interchain coupling and induce a transition from insulator to metal in polymers.[5,22] As a result, pressure modulation is usually implemented on chemically modified compounds to further develop metallic states. It is thus anticipated that taking advantage of electrostatic doping combined with pressure could be used to further enhance conductivity. However, such combined control of carrier doping and high pressure was difficult to be implement until the success of EDL gating with IL. Now, the liquid properties of IL could be further exploited as a medium for reaching a metallic state at high pressure along with high-efficiency EDL gating.

In this work, we present a newly developed gating-while-pressurizing process to merge the merit of both field effect doping and high pressure. Namely the ionic liquid used for charge accumulation also acted as the pressure media. Using this combination, we studied the transport properties of poly(2,5-bis(3-tetradecyl-thiophene-2-yl)thieno[3,2-b]thiophene) (pBTTT-C14) thin polymer film with two well controlled physical parameters: gate voltage (V_G) and pressures (P). At V_G = –3 V and a P = 2 GPa, the polymer reached a high conducting state with a 300 K dc-conductivity of 180 S cm^{-1} in a transistor configuration. A crossover from Mott variable range hopping (VRH)[23] to Efros-Shklovskii variable range hopping (ES-VRH)[24] was observed when cooling the device down to low temperatures (≈9.4 K at a P = 2 GPa) showing a clear sign of entering the regime adjacent to the metal–insulator (M–I) transition.[3,5] The crossover

Dr. W. Shi, Dr. J. T. Ye, Dr. J. G. Checkelsky, Prof. Y. Iwasa
Quantum-Phase Electronics Center and Department of Applied Physics
University of Tokyo
7–3–1 Hongo, Bunkyo-ku
Tokyo, 113–8656, Japan
E-mail: iwasa@ap.t.u-tokyo.ac.jp
Dr. C. Terakura, Prof. Y. Iwasa
Center for Emergent Matter Science
RIKEN, Hirosawa 2–1, Wako, 351–0198, Japan

DOI: 10.1002/adfm.201302954

is shifted to low temperatures by increasing pressure indicating enhanced inter-chain coupling, which is similar to behavior observed in chemically doped polypyrrole under high pressure preceding the eventual M–I transition.[5,22] These results clearly demonstrate an effective and reversible way to tune the transport of polymer semiconductors via a combined voltage and pressure control.

2. Results and Discussion

2.1. Ionic Liquid Gated Transistor of Polymer Thin Film

In order to realize a metallic state, we chose the conjugated polymer pBTTT-C14, as it showed a high mobility by a well established solution process for high device performance.[25,26] As discussed in detail in the experimental section, a careful tuning of the spin-coating process enabled preparation of a high quality thin film of pBTTT-C14 on a SiO_2/Si wafer with a smooth surface profile as shown in **Figure 1**a. The tapping mode atomic force microscopy (AFM) image showed a root-mean square of roughness of approximately 0.9 nm (for a total thickness of 36 nm measured from the height profile shown in Figure 1b). To confirm the microstructure of the thin film, we measured the out-of-plane X-ray (Cu Kα, 8 keV) diffraction. As plotted in Figure 1c, the peaks at the angle of 3.8° and 7.5° reflect the *d*-spacing of a characteristic lamellar structure with planes oriented parallel to the substrate.[25] From the observed peak position indexed as (*h*00), we estimated that the *d*-spacing along alkyl stacking direction is approximately 23 Å, which is consistent with previous reports.[27] After spin-coating and annealing, the microcrystalline pBTTT-C14 domains tend to orient in the lamellar structure with respect to the substrate as illustrated schematically in Figure 1d.

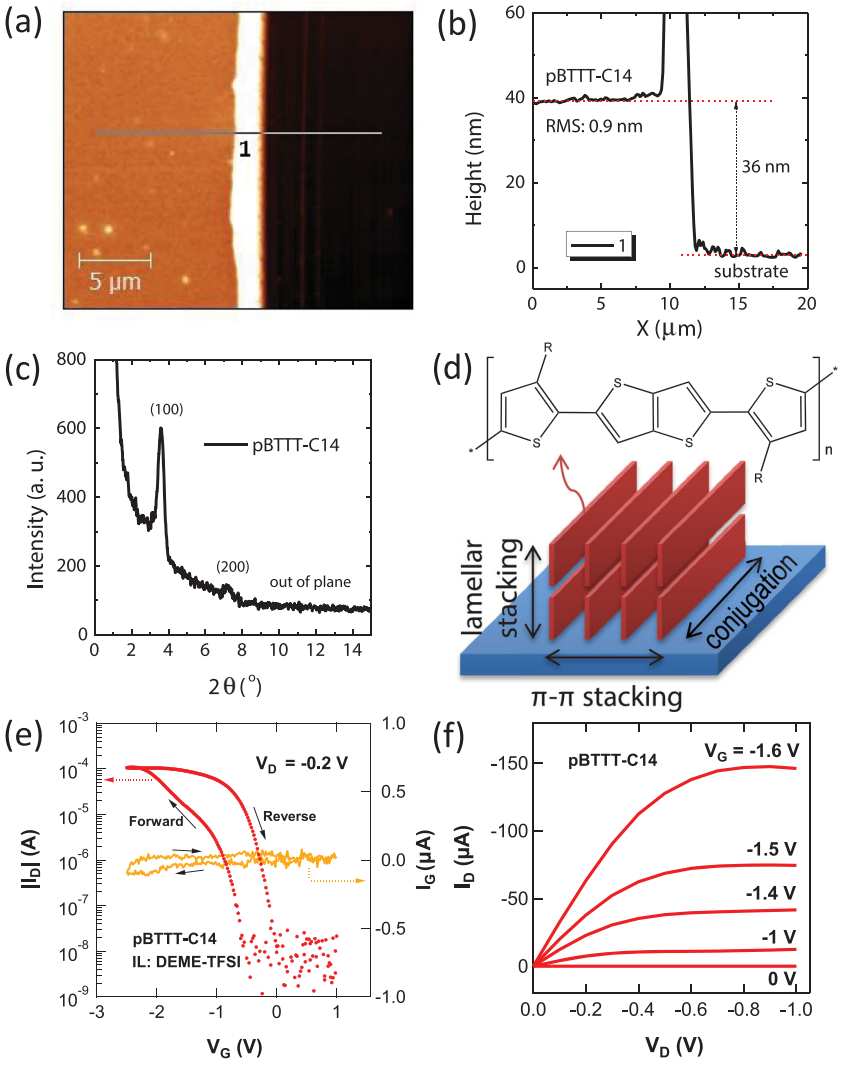

Figure 1. Structural characterization of pBTTT-C14 thin film and its transistor performance with ionic liquid gating. a) AFM image of a pBTTT-C14 thin film (brown region in the left) spin coated on a SiO_2/Si substrate after annealing at 180 °C. b) Height profile along the white horizontal line in (a). The thickness of the film is 36 nm and the RMS roughness is 0.9 nm. c) Out of plane X-ray diffraction of the pBTTT-C14 thin film on SiO_2/Si substrate showing (*h*00) scattering. d) Schematic illustration of the lamellar structure of the polymer thin film on the substrate. The molecular structure of pBTTT-C14 ($R = C_{14}H_{29}$) is shown at top of the panel. e) The gate voltage V_G dependence of the source-drain current I_D (red) and leakage current I_G (yellow) of a typical pBTTT-C14 thin film transistor device measured with drain voltage of –0.2 V at 300 K. The V_G was swept at a rate of 20 mVs^{-1}. f) The output characteristics (I_D versus V_D) of the same device measured with V_G from 0 V to –1.6 V.

Owing to high efficiency of IL as a gate dielectric, high-density carrier accumulation can be achieved by the formation of the EDL on the channel of EDL transistors. With the prepared thin films, we first confirmed such high transistor performance with EDL gating in several devices. Figure 1e and 1f show the transfer and output characteristics of a typical pBTTT-C14 TFT device measured at 300 K. The gate voltage was applied through the ionic liquid: N,N-Diethyl-N-methyl-N-(2-methoxyethyl) ammonium bis(trifluoromethanesulfonyl) imide (DEME-TFSI), which has been widely used in EDLT studies.[19–21] Under application of a small source-drain voltage V_{DS} = –0.2 V and sweeping V_G at a rate of 20 mVs^{-1}, we measured the drain current I_D and the gate leakage current I_G as a function of gate voltage V_G as plotted in Figure 1e. We note that I_G = –0.1 μA at V_G = –2.5 V, which is three orders magnitude smaller than the drain current I_D. The device displayed a typical *p*-type field effect transistor (FET) characteristic. The typical ON-OFF ratio was ~10^4, and in some devices reached ~10^5 with turn-on voltages of less than one volt in all devices. These parameters indicated a high device performance with EDL gating. A relatively large hysteresis caused by the slow ionic motion in the IL and the process of filling the trapping states was found similar to previous reports.[15,16] In Figure 1f,

the output curves showed linear and saturation behaviors by applying less than –1 V for V_D and –1.6 V for V_G. A large output current I_D up to 150 μA was observed even at V_G = –1.6 V, indicating that the whole thin film is doped by the ionic liquid rather than the initial EDL interface. This is likely due to the spaghetti-like polymer structure that introduces a high density of voids allowing small ionic liquid molecules to pass in the whole body of the thin film. However, the infiltration of IL into the polymer film, like a process of "bulk doping", did not disrupt the ordered structure in the polymer supported by the reversible behavior (as shown in Figure 1e) and the smooth increase of conductivity with gate (see **Figure 2**c). In our case, the entire film serves as the active channel, which is in stark contrast to the EDLTs using organic and inorganic single crystals.

2.2. Estimation of Carrier Density and Mobility

In order to estimate the carrier density and mobility of the ionic liquid-gated polymer thin film transistor, we carried out the capacitance measurement by electrochemical impedance spectroscopy (EIS). The capacitance of polymer film/ion liquid/Au structure was measured as a function of voltage at the frequency of 1 Hz. Since the surface of gold gate electrode is more than ten times larger than that of the polymer film, the total capacitance at the low frequency limit was approximately equal to the capacitance C of the polymer film/ion liquid interface.[28] Taking the measured capacitance shown in Figure 2a, the total charges accumulated in the polymer film at a given chemical potential V_G are obtained by integration of $C(V)$: $Q(V_G) = \int_0^{V_G} C(V)\,dV$. If $C(V)$ is in the unit per area, $Q(V_G)$ actually corresponds to the sheet carrier density n_s stored in the polymer film. Taking the film thickness of t = 36 nm, the bulk carrier density $n = n_s / t$, shown in Figure 2b. At V_G = –2.5 V, the estimated hole density was around 1.8×10^{20} cm^{-3}. As we know the conductivity $\sigma = ne\mu$, where e is the electron charge, then we can deduce the mobility μ at a given chemical potential. Figure 2c shows the channel conductivity as a function of gate voltages at room temperature for the same pBTTT-C14 device measured in Figure 1e. The conductivity reaches a maximum value of ~10^2 S cm^{-1} at V_G = –2.5 V. Here the conductivity is calculated assuming that the whole film is uniformly conducting. Noted that in some other reports, the conductivity is calculated by dividing the thickness of charge accumulation layer, which is only 1–2 nanometers for the EDL charges.[11,12] (If calculated in that way, the maximum conductivity of our pBTTT-C14 film reaches the order of 10^4 S/cm, which is comparable to their results.) Using the conductivity value in Figure 2c, the calculated mobility μ versus gate dependence V_G is plotted in Figure 2d. It is seen that μ increased from 0.003 cm^2 V^{-1} s^{-1} to 0.52 cm^2 V^{-1} s^{-1} as $|V_G|$ increases from –0.5 V to –1.0 V, which correlates well with the rapid increase of capacitance and conductivity initiating from the threshold voltage V_{th} = –0.5 V as indicated by the dashed vertical line in Figure 2. At V_G = –2.5 V, the mobility reached 2.7 cm^2 V^{-1} s^{-1}, which is significantly higher than that from conventional SiO_2-gated devices[25] but comparable with the carrier mobility measured in polymer electrolyte gated organic field effect transistors (OFETs).[12]

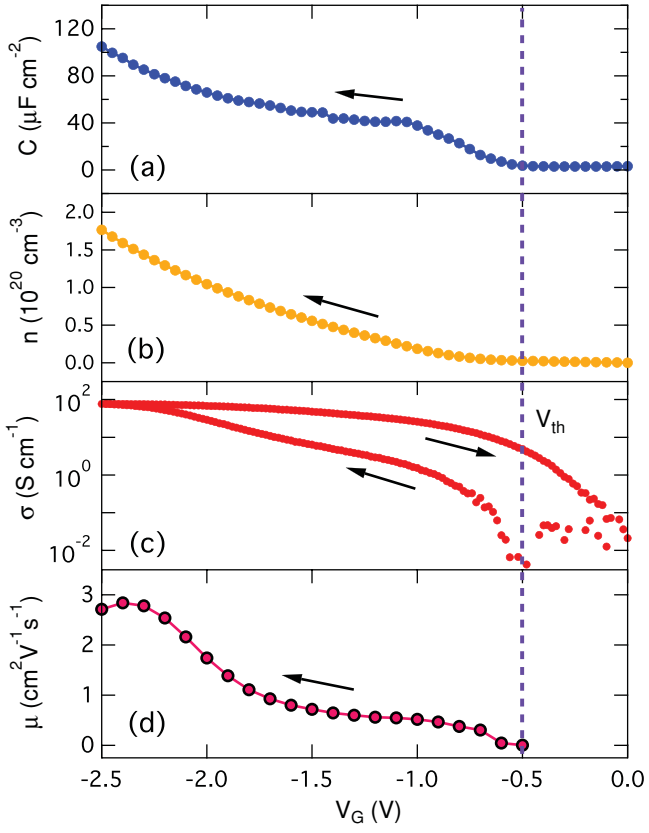

Figure 2. Gate voltage dependence of carrier density and mobility in a polymer EDLT device. a) The capacitance–voltage characteristics of a pBTTT-C14 thin film/ion liquid/Au structure at 1 Hz. b) Carrier density estimated by integration of capacitance versus gate voltage. c) Channel conductivity of the same pBTTT-C14 thin film device as shown in Figure 1e. d) The mobility versus gate voltage dependence calculated for the same device in (c). The arrows represent the sweeping directions of the curves. The dashed vertical line indicates the threshold voltage V_{th} of about –0.5 V for the charge transfer at room temperature.

2.3. Pressure Effect

Figure 3a schematically illustrates the conception of the gating-while-pressurizing technique utilizing the IL as both a gate and pressure media. Figure 3b–e shows optical images of the experimental setup for gating and pressurizing a pBTTT-C14 EDLT device. We used a hydrostatic pressure cell (see Figure 3b) with a Teflon cup (see Figure 3c) filled with IL. The polymer pBTTT-C14 transistor device (see Figure 3d,e) was sealed inside the Teflon cup and thus subject to the pressure applied via the liquid. Here, the typical inert liquid (Daphne oil) was replaced by IL as the pressure transmitting media. The front side of the wafer (Figure 3d) supported a typical 4-terminal polymer transistor with a bottom-contact configuration, whereas the back side of the wafer (Figure 3e) was attached to a large isolated platinum foil acting as the gate electrode. The pressure inside the cell at low temperature was calibrated by measuring the four-terminal resistance of a thin stripe of high purity lead through its superconducting transition temperature as shown

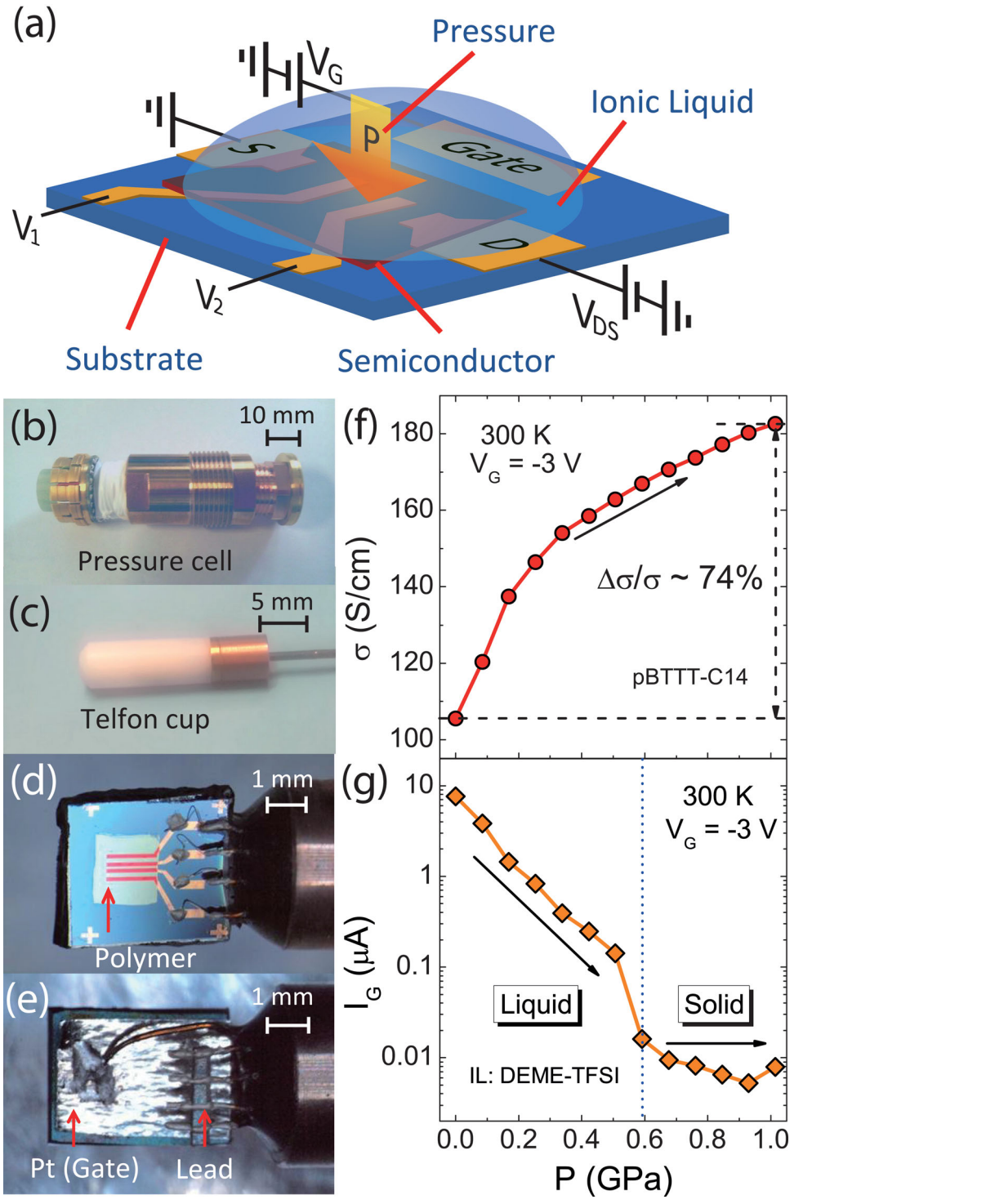

Figure 3. High pressure measurement setup and effect on polymer EDLT. a) A schematic of the 4-terminal IL-gated transistor device with external pressure applied through liquid medium of IL. b) A high pressure cell (model: HPC-33) for PPMS. c) A Teflon cup used inside the pressure cell serves as the container for IL: DEME-TFSI. d) Front side of a 4-terminal pBTTT-C14 EDLT device. The channel dimension was 1.2 mm (width) and 0.05 mm (length). e) Back side of the same device. A platinum foil was used as the gate electrode. The lead strip was used for calibration of the actual pressure at low temperatures by measuring its superconducting transition temperature. f) Conductivity σ at 300 K and fixed $V_G = 3$ V as a function of external pressure applied to the pBTTT-C14 thin film through the pressure cell using IL as the pressure medium. g) The leak current I_G as a function of external pressure. The dramatic decrease of I_G of one order of magnitude down to less than 20 nA under 0.59 GPa is an indication of phase change from liquid to solid of the DEME-TFSI.

in the Supporting Information, Figure S1. The relation between calibrated inner pressure and external load is provided in the Supporting Information, Figure S2a. The pressurization process is reversible despite some hysteresis caused by permanent deformation of the Telfon cup after the initial compression.

By sweeping V_G to –3 V, the dc-conductivity of pBTTT-C14 thin film transistor (TFT) at the ON-state reached a relatively high level of ~10^2 S cm^{-1} at 300 K after a saturation of I_{DS} at a V_G beyond –2.5 V as shown in Figure 1e. In order to further enhance the conductivity, we subsequently applied pressure onto the device with V_G fixed at –3 V using the pressure cell (Figure 3b). We plotted the 4-terminal dc-conductivity of a pBTTT-C14 TFT device as a function of external pressure applied at 300 K (Figure 3f), which clearly shows that the conductivity gradually increases further as the pressure increases. Quantitatively, we observed a 74% increase in conductivity achieved by increasing the external pressure P from 0 to 1 GPa. This pressure effect suggests that IL (DEME-TFSI) can be used as a pressure medium. Simultaneously, we recorded the leak current while applying P as shown in Figure 3g. The leak current showed a dramatic decrease by one order of magnitude when the external pressure was increased to critical value of P_c = 0.59 GPa (also see Supporting Information, Figure S2b). Above P_c, the I_G remained almost constant with further increase of P. If we keep $P > P_c$, the high conductivity states remained unchanged even after the removal of V_G. The observations above indicate that DEME-TFSI underwent a liquid-solid transition at P_c. On the other hand, as shown in Figure 3f, the conductivity of the polymer film continued to increase for $P > P_c$ without any appreciable anomaly at P_c. After freezing of ion movement at P_c, the carrier doping effect by V_G is maintained. Here, the continuous increase of conductivity is originated from a pure pressure effect. It is most likely to be attributed to reduction of the intermolecular distance of the polymer under pressure, creating greater π-orbital overlaps and thus enhancing carrier transport.[5,22,29,30] In other reports, optical studies on polymer and crystalline organic materials under pressure also revealed that the pressure indeed enhanced intermolecular coupling.[31–33] X-ray diffraction studies of polythiophenes have demonstrated that pressure of 8 GPa induced a 5–15% reduction in intermolecular distance.[34] To confirm whether this assumption applies to our system, we need future experimental studies by optical or X-ray characterization.[31–38] The application of ultra high pressure could cause irreversible changes to the polymer,[39] however it is suggested that the conjugated polymer chain can keep stable up to about 5 GPa,[34,39] a pressure significantly higher than the maximum used in our experiment (~2 GPa). Moreover, we observed a recovery of conductivity to the highly insulating state after pressure release (see Supporting Information, Figures S3, S4), suggesting that destructive effects of pressure on polymer structures are negligible in our case. It is worth noting that the pressure response of IL was no longer hydrostatic after its solidification. However, smooth change of the conductivity with P even after solidification indicate that a rubber like state of DEME-TFSI remained even at higher pressure region $>P_c$. On the other hand, the rubber state of IL at high pressure quenched the possibility of chemical reactions between IL and polymers regardless of the duration of applying high V_G at room temperature.

2.4. Transport properties

With applied V_G and P, we measured the temperature dependence of conductivity down to 2 K, which is plotted as log σ versus $T^{-1/2}$ and $T^{-1/4}$ in **Figure 4**a,b. (The original data is plotted in log scale in Supporting Information, Figure S5.) The red curves were measured by increasing the gate voltage V_G from –0.5 V to –2.0 V at P = 0 GPa. The blue curves correspond to σ (T) measured by applying the pressure from 0.09 GPa to 2.01 GPa at a fixed V_G = –3 V. Compared to the conductivity in previous reports using ion gel gated polymer measured at 300 K,[40] a doubled value of 180 S cm^{-1} was achieved with V_G = –3 V and P = 2.01 GPa.

The conduction mechanism at this highly doped state is characterized by variable range hopping (VRH). As shown in

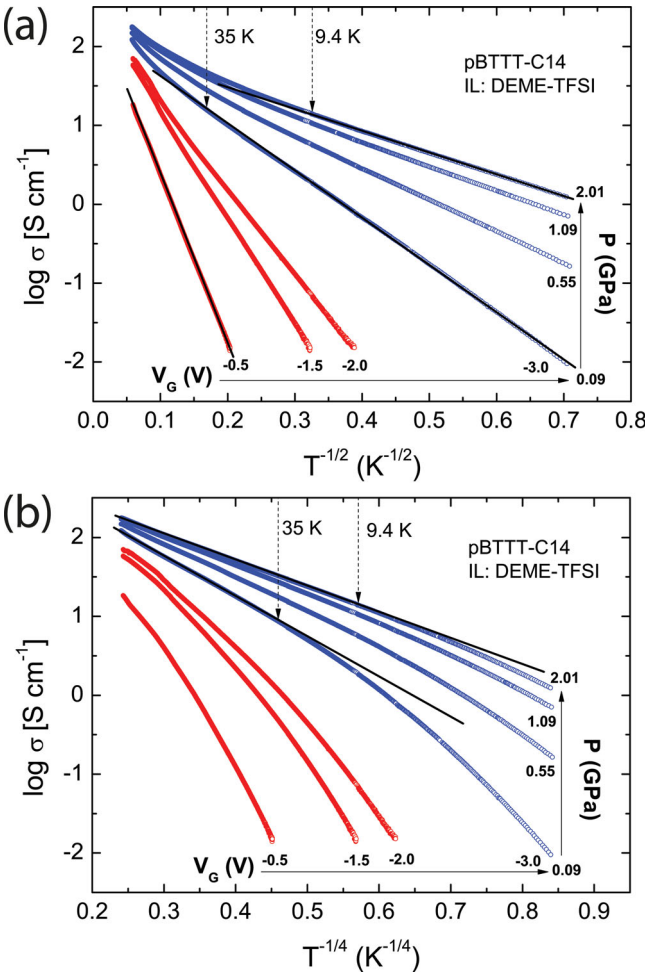

Figure 4. Transport characteristics of pBTTT-C14 thin film EDLT. a) The logarithm of conductivity plotted as a function of $T^{-1/2}$, appropriate for 1D-VRH conduction. b) The logarithm of conductivity plotted as a function of $T^{-1/4}$, appropriate for 3D-VRH conduction. The red curves were measured with V_G increasing from –0.5 V to –2.0 V, without applying pressure. The blue curves were measured with pressure increasing from 0.09 GPa to 2.01 GPa, with a fixed V_G = –3.0 V. The vertical dashed arrows indicate the crossover temperature from 3D to 1D-VRH for the high and low temperature regions, respectively. The solid straight lines are fits for different temperature ranges.

Figure 4, in a system dominated by VRH transport, the conductivity $\sigma(T)$ is described as:

$$\sigma\,(T) = \sigma_0 \exp\left[-\left(\frac{T_0}{T}\right)^{\frac{1}{n+1}}\right] \quad (1)$$

Here, n denotes the dimension of the system and T_0 is the VRH characteristic temperature.

From Figure 4a, we can see log σ follows linear with change of $T^{-1/2}$ over the entire temperature range for low gate bias V_G = –0.5 V. With the increase of V_G and P, the log σ versus $T^{-1/2}$ (n = 1) remains linear only at low temperature range (<9.4 K for the case under 2.01 GPa). Here, the system appears to cross into 1D hopping behavior described by Efros-Shklovskii (ES) VRH, where $\sigma = \sigma_{ES}\exp[-(T_{ES}/T)^{1/2}]$, with $T_{ES} = 2.8e^2/\varepsilon k_B L_c$ and ε is the dielectric constant.[24] For the high temperature range, instead, the log σ showed a linear relationship versus $T^{-1/4}$ (n = 3) as shown in Figure 4b. The 3D hopping behavior is identified as Mott VRH, where $\sigma = \sigma_{Mott}\exp[-(T_{Mott}/T)^{1/4}]$, with $T_{Mott} = 18/k_B L_c^3 N(E_F)$. Here, L_c is the localization length and $N(E_F)$ is the density of states at the Fermi level, E_F.[23] As compared in Figure 4a,b, a clear crossover from 3D-VRH to 1D-VRH conduction was observed in our device for high and low temperature region, respectively, as observed in chemically doped polypyrrole[3,5] and recently in ion-gel gated P3HT polymers.[40] And the crossover from Mott to ES type VRH is a clear signature that the polymer is in the regime close to the M–I transition.[3,5]

2.5. Hopping Analysis

For further characterizing the effect of V_G and P on the 3D-1D crossover in VRH, we analyzed the data by using a logarithmic derivative method (Zabrodskii plot),[41] in which logarithm of $d(\ln\sigma)/d(\ln T)$ is plotted as a function of $\ln T$ for linearizing $\sigma = \sigma_0 \exp[-(T_0/T)^x]$, where the slope obtained gives the value of x corresponding to $1/(n+1)$. As shown in **Figure 5**a, the solid lines represent three different regimes with slopes x = 0, 1/4, and 1/2, which coincide well with the data curves. Note that the exact linear fits to the three regimes gave the consistent parameters (see details in Supporting Information, Figure S6a). The zero slope (x = 0) observed at high temperature range corresponds to the critical regime which follows the power law dependence, $\sigma \propto T^{\beta}$, where $\beta = d(\ln\sigma)/d(\ln T)$. As the system approaches the M-I transition, β decreases from 1 to 1/3 in chemically doped polymers.[3,5] Here, β decreases from 0.83 to 0.56 as the P increased from 0.09 GPa to 2.01 GPa. With the increase of P, the temperature range covered by of this critical regime (x = 0) became wider. The power law dependence is also verified by a linear fit of log σ versus log T in the high temperature regimes (see Supporting Information, Figure S6b). From the blue curves with V_G = –3.0 V in Figure 5a, we can clearly see the slope change from x = 1/4 to 1/2, which again confirmed the crossover from Mott to ES VRH. The crossover temperature T_{cross} can be determined from the intersections of slopes with x = 1/4 and 1/2, which is marked by the vertical dashed lines. We plot T_{cross} as a function of P in Figure 5b, denoted by the black solid squares. At V_G = –3.0 V, T_{cross} shifted from 35 K to 9.4 K as

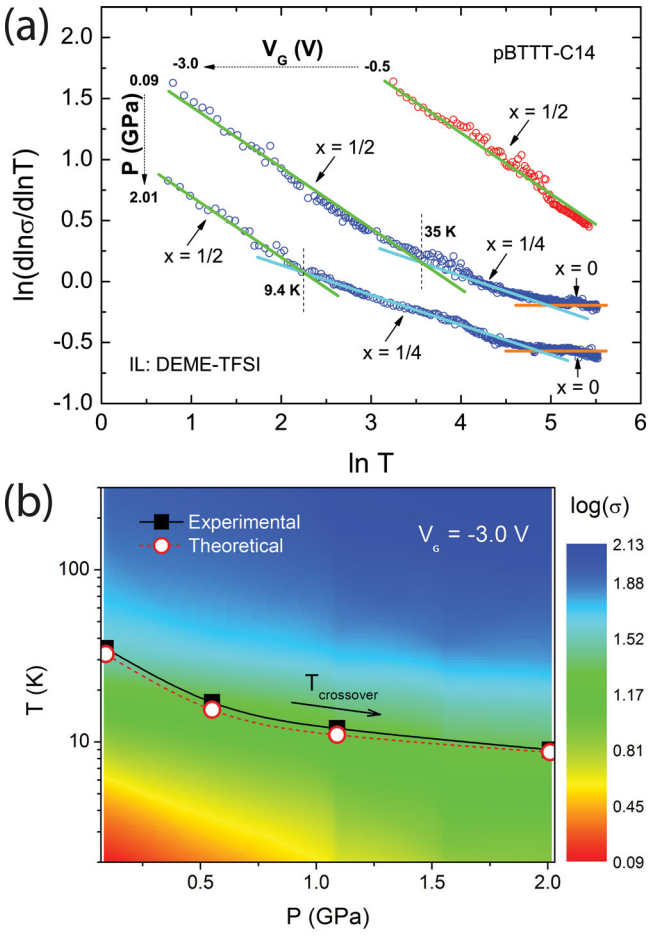

Figure 5. Hopping conduction analysis of transport as a function of gate voltage and pressure. a) Plot of $\ln(d(\ln\sigma)/d(\ln T))$ as a function of $\ln T$ for the curves shown in Figure 4. The solid lines represent three different regimes with slopes of x = 0 (orange), 1/4 (cyan), and 1/2 (green). The dashed vertical lines indicate the crossover temperatures at the intersections. b) The crossover temperature T_{cross} from Mott to ES VRH as a function of pressure. A good agreement was found between the black solid squares (experiment) and red open squares (theory, $T_{cross} = 16T_{ES}^2/T_{Mott}$). The color background is the 2D interpolated plot of log σ as a function of temperature and pressure with a fixed gate voltage V_G = –3.0 V.

P increases from 0.09 GPa to 2.01 GPa. The red open circles representing the predicted crossover temperatures calculated from the formulation $T_{cross} = 16T_{ES}^2/T_{Mott}$[3] are in good agreement with the experimental data, which strongly supports the interpretation of the crossover between Mott and ES VRH conduction. The color background in Figure 5b shows log σ in the 2D plane as a function of both T and P at a fixed V_G = –3.0 V. The crossover (both theoretical and experimental curves) appeared at the color region where the conducting states showed clear changes following the general trend of decrease of T_{cross} with increase P. This is consistent with the enhanced conductivity approaching metallic behavior (where the T_{cross} would approach zero). At P = 2.01 GPa, the conductivity ratio $\sigma(300\text{ K})/\sigma(2\text{ K})$ = 140. We expect that further increase of P using other techniques capable of generating higher pressures (e.g., diamond

anvil cell) will further reduce the conductivity ratio, which could eventually drive the polymer through the M–I transition.

3. Conclusions

In summary, we have demonstrated that ionic liquid DEME-TFSI can be used as a pressure medium as well as a gate dielectric. By using the newly developed gating-while-pressurizing technique, we investigated the transport properties of the conjugated polymer semiconductor pBTTT-C14 under a combined control of gate voltage and high pressure. The crossover from Mott to ES VRH transition was observed and shifted to low temperatures with the increase of gate voltage and pressure as a clear indication that the polymer has accessed the regime adjacent to the M–I transition and is approaching the metallic state. This combined technique, which enables a fine and reversible tuning of both high carrier densities and high pressure, may be a powerful tool for investigating a broad range of materials.

4. Experimental Section

Device Fabrication: The bottom contacted electrical leads of the polymer thin film transistor (TFT) device was prepared by evaporating a multilayer of metal of Ti/Au (5/60 nm) on a piece of SiO_2/Si wafer (0.3 cm × 0.4 cm). The polymer was spin coated on the prepared substrates at 1000 rpm in a nitrogen gas filled glove box from a warm solution (80 °C) of pBTTT-C14 dissolved in 1,2-dichlorobenzene (10 mg mL^{-1}). The polymer films were annealed at 180 °C for 30 min inside the glovebox before being mounted in the pressure cell and electrically connneted with feedthrough wires (Figure 3d). A platinum foil and a lead strip were then fixed and electrically wired at the backside of the substrate (Figure 3e). Ionic liquid: N,N-Diethyl-N-methyl-N-(2-methoxyethyl) ammonium bis(trifluoromethanesulfonyl) imide (DEME-TFSI) was filled in a Teflon cup (Figure 3c). The polymer transistor was immerged in the ionic liquid and sealed by the Teflon cup before being assembled into a pressure cell (Figure 3b) between a pair of pistons.

Pressure Calibration: An external force from an oil hydraulic cylinder was applied to the piston cylinder-type high pressure cell (Figure 3b) at room temperature. After cooling down the pressure cell to low temperatures, we measured the resistivity of a thin stripe of lead to determine its superconducting transition temperature T_c. The exact value of pressure can be determined from an established pressure dependent of T_c of lead.

Capacitance Measurement: The capacitance was measured by electrochemical impedance spectroscopy (EIS) on a polymer film/ion liquid/Au structure with polymer surface area much smaller than the Au surface area. An Electrochemical Workstation IM6eX (ZAHNER-Elektrik Gmbh & CoKG) was used to obtain the DC voltage dependence of capacitance at 1 Hz with the application of an ac voltage amplitude of 10 mV.

Transport Measurement: All electrical transport measurements were performed in a physical property measurement system (Quantum Design) using a Keithley 2182A nanovoltmeter and a 2612A sourcemeter. A small DC source-drain voltage ($|V_{SD}|$ = 0.1 V) was used to avoid possible Joule heating and non-linear response in the device at low temperatures.

Supporting Information

Supporting Information is available from the Wiley Online Library or from the author.

Acknowledgements

The authors thank Alberto Salleo for helpful suggestions on polymer semiconductors. This research was supported by Strategic International Collaborative Research Program (SICORP), Japan Science and Technology Agency, Grant-in-Aid for Scientific Research (S) (No. 21224009), for Specially Promoted Research (No. 25000003), and the "Funding Program for World-Leading Innovative R&D on Science and Technology (FIRST Program)" from JSPS, Japan.

Received: August 23, 2013
Revised: September 29, 2013
Published online: November 27, 2013

[1] C. K. Chiang, C. R. Fincher, Y. W. Park, A. J. Heeger, H. Shirakawa, E. J. Louis, S. C. Gau, A. G. MacDiarmid, *Phys. Rev. Lett.* **1977**, *39*, 1098.
[2] L. Zuppiroli, M. Bussac, S. Paschen, O. Chauvet, L. Forro, *Phys. Rev. B* **1994**, *50*, 5196.
[3] C. O. Yoon, M. Reghu, D. Moses, A. J. Heeger, Y. Cao, T.-A. Chen, X. Wu, R. D. Rieke, *Synth. Met.* **1995**, *75*, 229.
[4] Z. Wang, C. Li, E. Scherr, A. MacDiarmid, A. Epstein, *Phys. Rev. Lett.* **1991**, *66*, 1745.
[5] C. Yoon, R. M. D. Moses, A. Heeger, *Phys. Rev. B* **1994**, *49*, 10851.
[6] K. Lee, S. Cho, S. H. Park, A. J. Heeger, C. W. Lee, S. H. Lee, *Nature* **2006**, *441*, 65.
[7] R. Menon, C. Yoon, D. Moses, A. Heeger, Y. Cao, *Phys. Rev. B* **1993**, *48*, 17685.
[8] M. J. Panzer, C. D. Frisbie, *J. Am. Chem. Soc.* **2005**, *127*, 6960.
[9] H. Shimotani, G. Diguet, Y. Iwasa, *Appl. Phys. Lett.* **2005**, *86*, 022104.
[10] M. J. Panzer, C. D. Frisbie, *Appl. Phys. Lett.* **2006**, *88*, 203504.
[11] M. J. Panzer, C. D. Frisbie, *Adv. Funct. Mater.* **2006**, *16*, 1051.
[12] A. S. Dhoot, J. D. Yuen, M. Heeney, I. McCulloch, D. Moses, A. J. Heeger, *Proc. Natl. Acad. Sci. U. S. A.* **2006**, *103*, 11834.
[13] J. D. Yuen, A. S. Doot, E. B. Namdas, N. E. Coates, M. Heeney, L. McCulloch, D. Moses, A. J. Heeger, *J. Am. Chem. Soc.* **2007**, *129*, 14367.
[14] J. Lee, M. J. Panzer, Y. He, T. P. Lodge, C. D. Frisbie, *J. Am. Chem. Soc.* **2007**, *129*, 4532.
[15] J. H. Cho, J. Lee, Y. Xia, B. Kim, Y. He, M. J. Renn, T. P. Lodge, C. D. Frisbie, *Nat. Mater.* **2008**, *7*, 900.
[16] J. Lee, L. G. Kaake, J. H. Cho, X.-Y. Zhu, T. P. Lodge, C. D. Frisbie, *J. Phys. Chem. C* **2009**, *113*, 8972.
[17] T. Uemura, M. Yamagishi, S. Ono, J. Takeya, *Appl. Phys. Lett.* **2009**, *95*, 103301.
[18] S. Ono, N. Minder, Z. Chen, A. Facchetti, A. F. Morpurgo, *Appl. Phys. Lett.* **2010**, *97*, 143307.
[19] H. T. Yuan, H. Shimotani, A. Tsukazaki, A. Ohtomo, M. Kawasaki, Y. Iwasa, *Adv. Funct. Mater.* **2009**, *19*, 1046.
[20] J. T. Ye, S. Inoue, K. Kobayashi, Y. Kasahara, H. T. Yuan, H. Shimotani, Y. Iwasa, *Nat. Mater.* **2009**, *9*, 125.
[21] J. T. Ye, Y. J. Zhang, R. Akashi, M. S. Bahramy, R. Arita, Y. Iwasa, *Science* **2012**, *338*, 1193.
[22] M. Reghu, C. O. Yoon, D. Moses, A. J. Heeger, *Synth. Met.* **1994**, *64*, 53.
[23] N. F. Mott, *Metal Insulator Transitions* 2nd ed, Taylor and Francis, **1990**.
[24] B. I. Shklovskii, A. L. Efros, *Electronic Properties of Doped Semiconductors* Springer-Verlag, Berlin, **1984**.
[25] I. McCulloch, M. Heeney, C. Bailey, K. Genevicius, I. Macdonald, M. Shkunov, D. Sparrowe, S. Tierney, R. Wagner, W. Zhang, M. L. Chabinyc, R. J. Kline, M. D. McGehee, M. F. Toney, *Nat. Mater.* **2006**, *5*, 328.

[26] A. Salleo, R. J. Kline, D. M. DeLongchamp, M. L. Chabinyc, *Adv. Mater.* **2010**, *22*, 3812.
[27] M. L. Chabinyc, M. F. Toney, R. J. Kline, I. McCulloch, M. Heeney, *J. Am. Chem. Soc.* **2007**, *129*, 3226.
[28] H. Shimotani, H. Asanuma, J. Takeya, Y. Iwasa, *Appl. Phys. Lett.* **2006**, *89*, 203501.
[29] D. D. Schroepfer, P. P. Ruden, Y. Xia, C. D. Frisbie, S. E. Shaheen, *Appl. Phys. Lett.* **2008**, *92*, 013305.
[30] Y. Okada, K. Sakai, T. Uemura, Y. Nakazawa, J. Takeya, *Phys. Rev. B* **2011**, *84*, 245308.
[31] T. Kaniowski, S. Niziol, J. Sanetra, M. Trznadel, A. Pron, *Synth. Met.* **1998**, *94*, 111.
[32] S.-C. Yang, W. Graupner, S. Guha, P. Puschnig, C. Martin, H. R. Chandrasekhar, M. Chandrasekhar, G. Leising, C. Ambrosch-Draxl, U. Scherf, *Phys. Rev. Lett.* **2000**, *85*, 2388.
[33] M. Chandrasekhar, S. Guha, W. Graupner, *Adv. Mater.* **2001**, *13*, 613.
[34] J. Mardalen, E. J. Samuelsen, O. R. Konestabo, M. Hanfland, M. Lorenzen, *J. Phys.: Condens. Matter* **1998**, *10*, 7145.
[35] J. P. Schmidtke, J.-S. Kim, J. Gierschner, C. Silva, R. H. Friend, *Phys. Rev. Lett.* **2007**, *99*, 167401.
[36] Q. G. Zeng, Z. J. Ding, X. D. Tang, Z. M. Zhang, *J. Lumin.* **2005**, *115*, 32.
[37] C. Martin, S. Guha, M. Chandrasekhar, H. Chandrasekhar, R. Guentner, P. Scanduicci de Freitas, U. Scherf, *Phys. Rev. B* **2003**, *68*, 115203.
[38] M. A. Loi, A. Mura, G. Bongiovanni, Q. Cai, C. Martin, H. Chandrasekhar, M. Chandrasekhar, W. Graupner, F. Garnier, *Phys. Rev. Lett.* **2001**, *86*, 732.
[39] A. Brillante, M. Hanfland, K. Syassen, J. Hocker, *Physica* **1986**, *139* & *140B*, 533.
[40] S. Wang, M. Ha, M. Manno, C. Daniel Frisbie, C. Leighton, *Nat. Commun.* **2012**, *3*, 1210.
[41] A. G. Zabrodskii, K. N. Zeninova, *Zh. Eksp. Teor. Fiz.* **1984**, *86*, 727.